Journal of Innovations in Engineering Education
JIEE 2026, Vol. 9, Issue 1.

https://doi.org/10.3126/jiee.v9i1.87114

THAPATHALI CAMPUS
Institute of Engineering
Tribhuvan University

A low-cost inertia-based chassis dynamometer for performance evaluation of two-wheeler CVT vehicles

Abiral Guni[a,b,*], Prajwal Raj Shakya[a,b], Sakar KC[a], Sanjaya Acharya[a] and Rohit Thapa[a]

[a]*Department of Automobile and Mechanical Engineering, Thapathali Campus, Institute of Engineering, Tribhuvan University, Kathmandu, Nepal*

[b]*Department of Mechanical and Aerospace Engineering, Pulchowk Campus, Institute of Engineering, Tribhuvan University, Lalitpur, Nepal*

ARTICLE INFO

Article history:

Received 6 December 2025
Revised in 26 February 2026
Accepted 18 April 2026

Keywords:

Chassis dynamometer
Inertia-based loading
Two-wheeler CVT
Brake power measurement
Vehicle performance testing

Abstract

Chassis dynamometers are an essential tool for controllable and repeatable evaluation of vehicle performance. However, commercial chassis dynamometers are expensive and often inaccessible to small laboratories and educational institutions. In this regard, this study presents the development and experimental evaluation of an inertia-based chassis dynamometer for two-wheeler vehicles with continuously variable transmissions (CVTs), achieved at a cost of under $500. The system uses a roller-flywheel assembly to simulate realistic drive-load conditions by translating the vehicle-rider translational inertia into an equivalent rotational inertia at the roller. Based on typical vehicle–rider mass characteristics of CVT scooters, a target system inertia of 1.80 kgm² was derived, while the fabricated assembly achieved 1.74 kgm². A Honda Dio (2015) was selected as the test vehicle based on availability, and its parameters fall within the intended design range. The brake power measurement at wheels was taken using a rope brake arrangement under steady-state conditions across a speed range of 0 – 41.55 km/h. Later, the results were validated against a commercial inertia dynamometer, which indicates that, although the fabricated dynamometer consistently underestimates brake power, both systems yielded similar power-speed trends with comparable linear slopes. And, the deviation between the datasets remained approximately constant across the speed range. Additionally, fuel economy measurements under inertia-only loading averaged at 35 km/l across urban speed ranges, approximately 13% below the real-world reported range of 40 – 45 kmpl.

1. Introduction

Chassis dynamometers are essential tools in the automotive space for evaluating vehicle performance, emissions, and fuel economy in a controlled environment that replicates road loads in a stationary setting. They are of interest because they allow measurement of performance at the driving wheels and therefore inherently capture drivetrain losses, tire-roller interaction effects, and transmission behavior. This capability makes chassis dynamometers useful for assessing brake power, torque characteristics, and fuel consumption in a repeatable manner, and entirely bypasses the variability associated with on-road testing [1][2].

Modern chassis dynamometer systems enable precise road-load simulation and steady-state operation by employing load-absorption units such as eddy-current, hydraulic, or electric dynamometers [3][4]. Moreover, these systems are integrated with sophisticated data acquisition and control systems that upgrade the functionality of chassis dynamometers to emission testing and certification, regulatory compliance testing, and vehicle development programs. But on the other hand, this brings complexity to the dynamometer system, and the cost of such facilities limits their accessibility to OEMs and specialized testing labs, thus making it unfeasible for smaller workshops, educational institutions, and resource-constrained research environments [3][5].

To address these limitations, several studies have showcased simplified and low-cost configurations, and an inertia-type chassis dynamometer is one of such ap-

*Corresponding author:
080msree002.abiral@pcampus.edu.np (A. Guni)

proaches. Inertia-type dynamometers consist of a roller-flywheel assembly that provides a known rotational inertia that resists vehicle acceleration, and ultimately, the power from the vehicle is deduced from measured speed or deceleration characteristics [1][4]. An obvious advantage that such dynamometers have over actively braked systems is their mechanical simplicity and the minimal infrastructure required. However, the accuracy of the result yielded by an inertia-based chassis dynamometer is heavily influenced by inertia matching, mechanical losses, and calibration approaches, which need to be carefully assessed to ensure a workable result [6][7].

There have been some notable studies demonstrating the feasibility of inertia-based and mechanically braked chassis dynamometers for light vehicles and two-wheelers. [8] developed a retarder-type chassis dynamometer for two-wheeler applications, but rather than accuracy, it emphasized repeatability and comparative performance evaluation. Similarly, [9] stretched the concept to electric two-wheelers and highlighted the continued relevance of roller-based dynamometers for small vehicles. Educational and lab-scale dynamometer systems such as [5] and [10] have also been reported, but they focus on affordability and transparency of design.

Replication of real-world road loads on a chassis dynamometer remains non-trivial. SAE J2263 mentions coast-down testing and standardized procedures for road load determination, but at the same time, it requires comprehensive instrumentation, a controlled environment, and data processing [4][11]. Then again, variability can still arise due to environmental conditions and measurement procedures in place [11]. Modeling approaches that account for tire-roller slip, aerodynamic effects, and dynamic load variations have been developed to improve the outcomes further, but those come with increased system complexity and cost [6][7][12].

For a simplified chassis dynamometer, particularly an inertia-based, two-wheeler vehicle equipped with continuously variable transmissions (CVTs), is a relevant application domain. CVT-based scooters comprise a fairly large portion of the overall two-wheeler market. Also, from a testing perspective, CVTs come with their own complexities because of their continuously varying ratio, slip behavior, and sensitivity to operating conditions [13][14]. In this regard, a chassis dynamometer can capture the wheel-side performance measurements, which, in turn, can offer insights that are beyond the scope of engine-only testing, given that the limitations of the measurement system are properly understood.

Within this context, the present study focuses on the design, fabrication, and experimental evaluation of a low-cost inertia-based chassis dynamometer with an auxiliary mechanical brake arrangement. Unlike studies [8][9][10], which primarily emphasize dynamometer design and functional testing, the presented work adopts a measurement-oriented approach by explicit inertia matching and comparative validation against a commercial inertia chassis dynamometer, and is designed specifically for two-wheeler CVT vehicles. Furthermore, this developed system is also made capable of measuring the fuel efficiency of the test vehicle.

Rather than introducing a new dynamometer principle, the study focuses on establishing a transparent and cost-effective design methodology supported by explicit inertia matching and a simple parameter measuring mechanism whose results are later compared with a commercial inertia chassis dynamometer. The system is evaluated for its ability to deliver repeatable and representative results suitable for educational use and small-scale laboratory applications, with clear documentation of measurement uncertainty.

2. Material and methods

2.1. Test system overview

The constructed dynamometer is based on the principle of simulating road-load conditions by requiring the test vehicle to accelerate a mass of known inertia. Brake power and fuel consumption can then be determined by measuring the rotational speed and braking force during operation. Unlike a pure inertia dynamometer, which measures power at wheels by measuring the acceleration of the drive wheel [4], the developed system incorporates inertia components to simulate drive loads and employs a steady-state brake power evaluation mechanism (rope-brake mechanism) to measure power at wheels.

The rear wheel of the test vehicle is in contact with a cylindrical roller connected to a shaft-mounted inertia assembly. When the vehicle accelerates, the assembly rotates, generating resistance equivalent to the inertial load experienced under on-road conditions. A controlled braking force is applied through a mechanical rope brake setup, which allows the estimation of torque and power at the wheel. The configuration and layout of the developed system are shown in Figure 1, along with components: (1) Roller, (2) Flywheel, (3) Pulley for rope-brake mechanism, (4) Bearing, (5) Sheet Metal, (6) Front Wheel Restraint, while Figure 2 shows the fabricated setup.

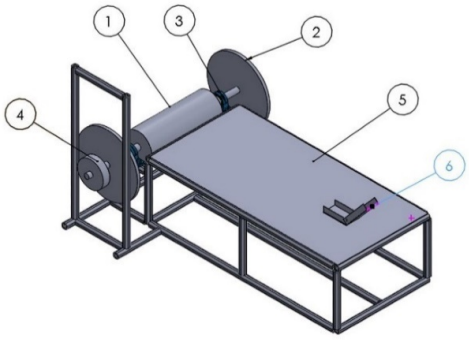

Figure 1: CAD model of the developed inertia chassis dynamometer

Figure 2: Fabricated dynamometer

2.2. System architecture and major components

The major components of the system are summarized below.

2.2.1. Roller-flywheel assembly

The roller is the primary interface between the test vehicle and the dynamometer, and it directly influences traction behavior and rotational dynamics. A cylindrical roller was selected with surface grooves to minimize slip during operations. The roller dimensions were chosen to ensure sufficient contact with the drive wheel, ease of machining and fabrication, and compatibility with the inertia requirements of the dynamometer.

Also, two flywheels of equal mass were mounted symmetrically on the shaft to achieve an overall inertial loading comparable to the scaled vehicle inertia. The use of flywheels provides a controllable means of increasing total system inertia without altering roller geometry or contact conditions.

2.2.2. Shaft and bearing support

The roller-flywheel assembly is mounted on a mild-steel shaft that is supported by pillow block bearings at both ends. The shaft transmits the torque generated by the drive wheel of the test vehicle while ensuring stable rotation of the inertia assembly.

2.2.3. Load application mechanism

A rope brake mechanism was integrated into the dynamometer system to apply braking resistance on the rotating shaft. The braking force was measured using a spring balance, which allowed further calculation of torque and brake power.

2.2.4. Structural frame and vehicle support

All components were mounted on a welded mild-steel frame that supported the dynamometer assembly and the test vehicle. A sheet metal was provided over the frame to support the mounted vehicle. A front-wheel restraint was welded to a structural member of the frame to prevent longitudinal motion of the test vehicle during testing.

2.2.5. Instrumentation

The rotational speed of the shaft was measured using a digital tachometer, and the braking force was obtained via the rope brake-spring balance arrangement.

2.3. Measurement model and governing equations

The adopted measurement model establishes relationships between the total vehicle mass, roller geometry, flywheel inertia, and measured parameters to effectively reproduce representative dynamic loading conditions. The governing equations discussed in the following subsections define the effective vehicle inertia, how that inertia is transformed into the roller reference frame, and the total amount of inertial loading experienced by the dynamometer.

2.3.1. Effective vehicle inertia

For a two-wheeler tested on a roller-type inertia dynamometer, the vehicle–rider translational mass can be represented as an equivalent rotational inertia at the driven wheel, assuming pure rolling contact [15]. Assuming the total mass of the vehicle (including rider) as M and radius of the driving wheel as R, the equivalent inertia is given by Equation 1.

$$I_{\text{vehicle}} = M R^2 \tag{1}$$

2.3.2. Roller inertia

The rotational inertia of the hollow cylindrical roller is given by Equation 2. Here, m is the mass of the roller, while r is the radius of the roller.

$$I_{\text{roller}} = \frac{1}{2}mr^2 \tag{2}$$

2.3.3. Gear ratio adjustment

Since the drive wheel diameter exceeds the roller diameter, a geometric scaling factor was introduced to relate the vehicle-side inertia to the roller-side inertia. This scaling accounts for the difference in angular velocity between wheel and roller and allows the equivalent inertial load to be reduced to the dynamometer reference frame. This measure was obtained through Equation 3.

$$\text{Gear Ratio (G.R.)} = \frac{\text{Diameter of drive wheel}}{\text{Diameter of roller}} \tag{3}$$

The equivalent inertia required at the roller is given by Equation 4, obtained through Equations 1 and 3.

$$I_{\text{required}} = \frac{I_{\text{vehicle}}}{\text{G.R.}} \tag{4}$$

2.3.4. Flywheel contribution

As mentioned in Section 2.2.1, the roller-only inertia was not sufficient to simulate the required inertia loading. So, two identical-sized flywheels of mass m_1 and radius r_1 were used, whose total inertia was calculated via Equation 5.

$$I_{\text{flywheel}} = m_1 r_1^2 \tag{5}$$

2.3.5. Total effective inertia of the dynamometer

Under the proposed design of the inertia-based dynamometer system, the total inertial loading is a sum of the inertia of the roller and that of the flywheels, as showcased by Equation 6.

$$I_{\text{Dyno}} = I_{\text{roller}} + I_{\text{flywheel}} \tag{6}$$

2.4. Test vehicle and parameters

Experimental testing was conducted using a widely available CVT-equipped two-wheeler scooter. The key vehicle parameters and derived quantities used in the dynamometer design are summarized in Table 1.

2.5. Mechanical design and verification

The design of the inertia chassis dynamometer was carried out to ensure a rigid structure, safe torque transmission, and stable operating conditions under the representative testing conditions.

2.5.1. Shaft design

Under combined loading, shaft sizing was performed using the standard rotating shaft design, and based on the calculated equivalent torque and allowable stress, a shaft diameter of 22 mm was selected. Furthermore, verification of the shaft under static loading was performed using finite element analysis in ANSYS APDL, where the bending moment distribution (Figure 4), shear force variation (Figure 5), and deflection characteristics (Figure 6) were examined. The analysis confirmed that stresses remained within allowable limits, shaft deflection was minimal under operating load, and the selected diameter provided sufficient stiffness.

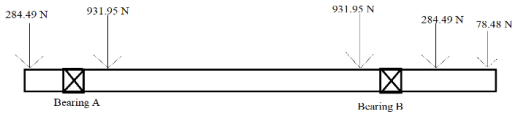

Figure 3: Free-body diagram of stationary loading conditions on the shaft

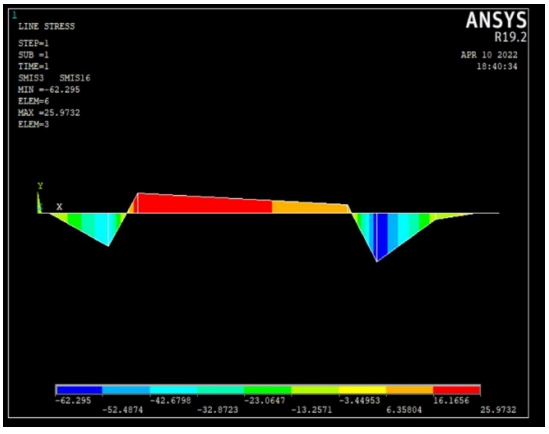

Figure 4: Bending moment distribution along the shaft

Figure 5: Shear force distribution along the shaft

Table 1: Test vehicle specifications and derived parameters

Parameter	Symbol	Value	Description
Vehicle Type	–	CVT Scooter	Honda Dio 2015 Model
Total Vehicle Mass	M	165 kg	Vehicle mass including rider
Wheel Diameter	D_{wheel}	0.44 m	–
Wheel Radius	R	0.22 m	–
Roller Diameter	D_{roller}	0.21 m	–
Roller Radius	r	0.105 m	–
Gear Ratio	G.R.	2.1	Equation 3
Effective Vehicle Inertia	I_{vehicle}	8 kgm^2	Equation 1
Required Inertia Loading	I_{required}	1.8 kgm^2	Equation 4
Roller Inertia	I_{roller}	0.143 kgm^2	Equation 2
Flywheel Inertia	I_{flywheel}	1.596 kgm^2	Equation 5
Total System Inertia	I_{dyno}	1.74 kgm^2	Equation 6

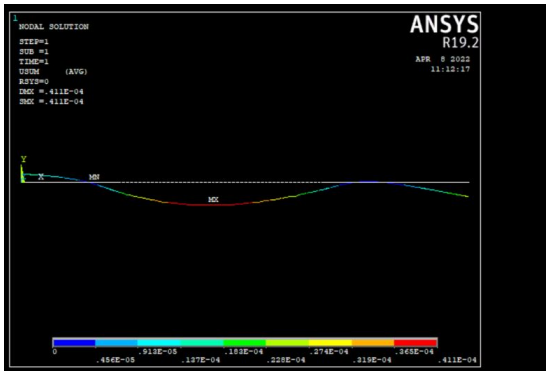

Figure 6: Shaft deflection profile under static loading conditions

2.5.2. *Bearing selection*

Based on the calculated radial loading acting on the shaft due to the assembly and transmitted forces, UCP 208 pillow block bearings were used. The minimum required dynamic load rating for safe operation was determined as $C_{10,\text{required}} = 20.19$ kN. So, based on this and market availability, the UCP 208 pillow block was selected.

2.5.3. *Frame design*

The frame was fabricated using mild-steel square sections of $1.5'' \times 1.5'' \times 0.25''$, and the surface for mounting the test vehicle was provided by a steel sheet platform welded to the frame. Structural verification was performed using finite element analysis in ANSYS Fluent under calculated loading conditions. The analysis reported a maximum bending moment of 69.256 Nm (Figure 7) and a maximum deformation of 0.04 mm (Figure 8) under the applied loading condition. The bending capacity of the selected tube section was estimated using Equation 7.

$$M_{\text{allowable}} = \sigma_{\text{allow}} \cdot Z \tag{7}$$

Where Z is the section modulus of the tube, and σ_{allow} is the allowable bending stress for mild steel. The value of Z for the square section tube was calculated to be 7397 mm^3 while the σ_{allow} was taken as 125 MPa as a conservative working value. This gives an allowable bending moment capacity of 923 Nm, which is significantly higher than the FEA demand. Moreover, the allowable deflection was calculated to be 3.33 mm, which also indicates the frame is far safer than the FEA indicated limit.

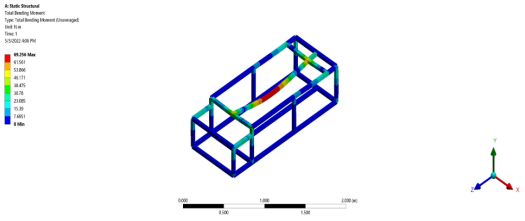

Figure 7: Finite element bending moment distribution of the dynamometer frame

2.6. Materials sourcing and fabrication approach

The dynamometer was built from both newly purchased components and recycled industrial materials. The rotating components of the system, such as the rollers, flywheels, and the sheet metal to support the vehicles being loaded, were made from reclaimed steel stock taken from the dismantled machinery and surplus sup-

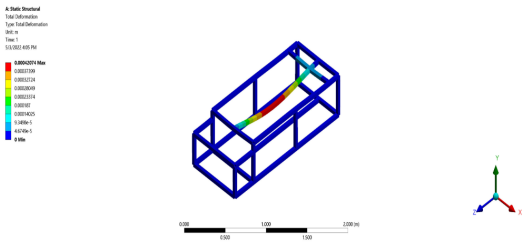

Figure 8: Total deformation of the frame under full loading

plier sources. But the critical load-bearing and precision components, i.e., structural frame members, shaft, and bearings, of the dynamometer were new to ensure dimensional accuracy, mechanical stability, and safe operation. The shaft was machined to the required dimensions using lathe operations before assembly, and new pillow block bearings were selected based on calculated load requirements.

The total cost to develop the dynamometer was kept below $500, significantly lower than that of commercial chassis dynamometers used for two-wheeler testing. This figure also supports the intended application of the system for educational and small-scale laboratories.

2.7. Instrumentation and data acquisition

Keeping simplicity, cost-effectiveness, and compatibility in mind, the measurement of performance parameters from the dynamometer was carried out using a combination of mechanical and digital instruments. The rotational speed (N) of the roller-shaft assembly was measured through the shaft using a digital non-contact tachometer. During operation, the braking force was applied through a rope wound around the pulley drum of radius R, with one end attached to a tray where known weight plates (W) were applied, and the other end was connected to a spring balance. The difference between the applied weight and the spring balance reading (S) provided the net braking force acting on the pulley. All measurements were recorded under steady operating conditions, and brake power (BP) values were computed for each test point using Equation 8.

$$BP = \frac{2\pi N(W - S)R}{60} \tag{8}$$

Fuel consumption tests were conducted using a volumetric method in which the fuel usage was recorded over a fixed operating duration under steady conditions.

3. Results and discussion

3.1. Brake power characteristics of the fabricated dynamometer

The brake power was evaluated across a speed range of 0 to 41.55 km/h, shown in Figure 9, which illustrates the relationship between brake power and speed for the developed dynamometer. The observed trend follows the expected theoretical behavior: brake power increases approximately in proportion to rotational speed under increasing load. The maximum power at the wheels was observed to be 0.35 kW at the highest tested speed. The slight non-linearity in the mid-speed range can be attributed to the CVT, which adjusts the transmission ratio and alters torque multiplication characteristics.

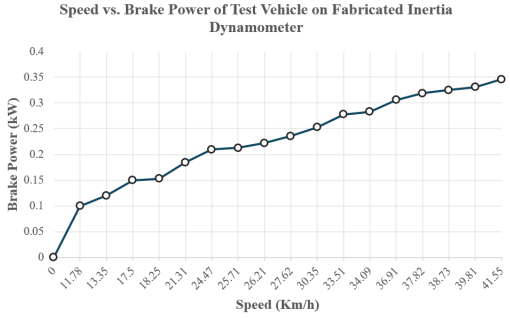

Figure 9: Variation of brake power with wheel velocity obtained from the fabricated inertia dynamometer

3.2. Comparison with the standard inertia dynamometer

To validate the measurement, the obtained results were compared against a standard inertia dynamometer (MSR 400 VP 630012, MAHA, Haldenwang, Germany), which measures wheel power with an accuracy of approximately ±2% [16]. As shown in Figure 10, the fabricated dynamometer consistently underestimates brake power relative to the standard dynamometer.

The maximum power reading obtained from the standard inertia dynamometer was 0.84 kW at 63.43 km/h. For a comparative standpoint, a reading was observed at 43.29 km/h, where the indicated power at wheels was 0.51 kW, whereas the power output at 41.55 km/h measured from the fabricated dynamometer was 0.35 kW.

Linear trendlines fitted to both datasets yield slopes of 0.0081 kW/(km/h) ($R^2 = 0.9987$) and 0.009 kW/(km/h) ($R^2 = 0.9182$) for the fabricated and standard dynamometers, respectively. This indicates

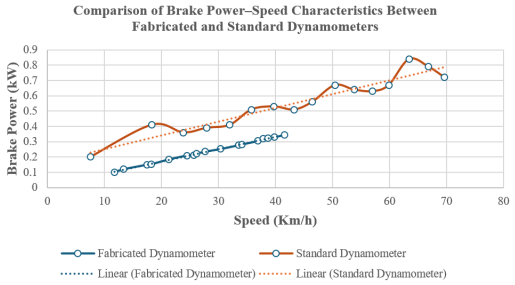

Figure 10: Comparison of brake power obtained from the fabricated inertia dynamometer and the commercial eddy-current dynamometer

that both systems exhibit a comparable rate of power increase with speed and suggests that the fabricated dynamometer reliably captures the underlying performance trend. Moreover, the difference between the two datasets is mainly characterized by a consistent offset across the operating range rather than by a change in trend.

While the fabricated dynamometer does not capture transient fluctuations due to its steady-state measurement approach, it demonstrates stable and repeatable performance with a well-defined linear response. The underlying causes of the observed deviation are discussed in detail in Section 3.3.

3.3. Discrepancy between fabricated and standard inertia dynamometer

The deviation in the power-speed curve between the fabricated dynamometer and the commercial inertia dynamometer arises from the differences in measurement approach, internal loss compensation mechanism, and dynamic data acquisition. The fabricated dynamometer estimates the power at the wheels using a mechanical rope-brake absorption method and does not compensate for losses that are dissipated within the rope-brake interface.

Moreover, additional discrepancies come from tire-roller interaction differences. The MAHA MSR 400 employs a large diameter roller (400 mm) with precision surface characteristics [16], while the fabricated system uses a smaller mild-steel roller (210 mm) with a rugged finish. [7] show that roller diameter significantly affects tire-roller contact behavior and rolling resistance, with deformation, slip interaction, and hysteresis contributing to energy losses in chassis dynamometer testing.

Post-processing corrections for tire-roller geometry, such as rolling resistance adjustments based on roller radius ratios proposed in [6] could partially reduce the numerical discrepancy between the fabricated and reference results. However, such corrections introduce additional modeling assumptions and calibration dependencies, so no corrections were applied to preserve methodological transparency and ensure that reported measurements reflect the intrinsic behavior of a low-cost fabricated system.

Also, a noteworthy thing in the nature of the data of the standard inertia dynamometer is the local peaks and dips seen in the power curve in Figure 10. This indicates the capability of the MAHA system to capture transient fluctuations caused by CVT ratio variation and throttle response.

3.4. Fuel efficiency analysis

To measure the fuel efficiency of the test vehicle, separate quasi-steady test runs were conducted under five operating speeds spanning typical urban scooter usage. The test vehicle (Honda Dio 2015 model) was operated at steady velocities in the range of 24.2 to 45.6 km/h, and fuel consumption was measured for each run using a volumetric method in which the engine was supplied from an external graduated fuel container. The reduction in fuel level was recorded immediately after the run to minimize evaporation losses. The distance for each run was obtained from dynamometer kinematics, and the mileage was calculated as the ratio of distance travelled and volume of fuel consumed. The engine was warmed up before the test, and throttle conditions were maintained throughout each test.

Moreover, the tests were performed at multiple urban driving speeds rather than at a single standardized speed to provide an evaluation of fuel economy as it relates to load and whether the inertially matched dynamometer produced realistic results.

The mileage results were combined and averaged across the full range of test operating conditions to generate an average fuel efficiency for the tested speed range. Table 2 presents the results of the fuel efficiency test.

The mileage measured under inertia-only loading ranged from 37 km/l at lower speeds to 31.67 km/l at higher speeds, averaging at $\tilde{3}5$ km/l. The real-world mileage for the test vehicle ranged from 40 to 45 kmpl. The deviation occurs since the aerodynamic and rolling resistance were not explicitly modeled in the efficiency test. Based on this, it can be concluded that the fabricated inertia-matched dynamometer provides a representative steady-state loading and does not inflate fuel-economy results.

Table 2: Fuel consumption and mileage results

Runs	Speed (km/h)	Distance (km)	Fuel (L)	Mileage (km/l)
1	24.2	2.0	0.054	37.04
2	28.6	2.3	0.065	35.38
3	33.5	2.8	0.080	35.00
4	37.3	3.1	0.090	34.40
5	45.6	3.8	0.120	31.67

3.5. Limitations and validation scope

Measurement and validation of the developed dynamometer were done using a single vehicle platform (Honda Dio, 2015 model). This provides initial verification of functional performance, but generalization across other engine displacements, vehicle masses, and CVT tuning requires further evaluation. Considering how drivetrain response and torque characteristics can vary across platforms, multi-vehicle validation would make the dynamometer more comprehensive and robust.

The maximum speed for the power test was 41.55 km/h, while that for the fuel efficiency test was 45.6 km/h. The speed range was deliberately limited due to laboratory and safety constraints associated with operating a single roller dynamometer without an enclosed test cell. Although these speed ranges adequately represent typical urban operating conditions for scooters, evaluation at higher speeds would enable assessment of the potential slip and nature of parasitic losses at elevated speed levels.

Also, while the observed performance trends indicate realistic CVT drivetrain behavior within the tested range, integration of a calibrated absorption mechanism or road-load simulation model would allow more accurate replication of real-world driving resistance, thus enhancing the accuracy of the developed system.

4. Conclusion

This work presented the design, fabrication, and experimental validation of an inertia-based chassis dynamometer, specifically for two-wheeler CVT vehicles. Although chassis dynamometers are inherently expensive due to the complexity of instrumentation, control systems, and calibration requirements, this study established that explicit inertia matching is a viable and explorable design basis for a low-cost alternative. Moreover, the working system was achieved within a budget of under $500, which makes it particularly suitable for educational and preliminary research uses.

While the system significantly underestimates brake power, yielding an overall mean deviation of 45.4% across the full common speed range compared with the MAHA MSR 400 commercial inertia dynamometer, the causes of this deviation are well recognized and understood as characteristic of simplified inertia-only dynamometer configurations. These deviations arise primarily from inherent limitations of the adopted measurement methodology, including unaccounted drivetrain losses, tire–roller slip, and the absence of active load control.

Future work should focus on upgrading the system by integrating controlled loading mechanisms or developing a roller–tire interaction correction model to compensate for slip and rolling resistance effects. The latter approach would enable more accurate estimation of absolute brake power while retaining the cost advantages and simplicity of the current design.

Fuel economy results under inertia-only loading average approximately 35 km/l across the speed range of 24 km/h – 45.6 km/h, against a manufacturer-reported real-world number of 40 – 45 km/l, which confirms that the dynamometer imposes realistic resistive loading without overestimating efficiency figures.

Acknowledgments

The authors declare that the work did not receive any external funding or a specific grant for this study. The research was carried out using available institutional facilities and personal resources.

Author contributions

Abiral Guni: Conceptualization, methodology, design, and fabrication of the dynamometer, data curation, analysis, and manuscript writing

Prajwal Raj Shakya: Supervision, project administration, and critical review of the methodology and manuscript

Sakar KC: Investigation, identification of the fabrica-

tion site, resource acquisition, and hands-on technical support during fabrication and testing

Sanjaya Acharya: Conceptualization, CAD design, and contributing to fabrication and manuscript writing

Rohit Thapa: Validation, data analysis, fabrication, and review of the manuscript

Conflict of interest

The authors declare that they have no conflict of interest.

Data availability

The data supporting the findings of this study are available from the corresponding author upon reasonable request.

References

[1] Hanapi S, Tijani A S, Rahim A H A, et al. Comparison of a prototype PEM fuel cell powertrain power demand and hydrogen consumption based on inertia dynamometer and on-road tests[J/OL]. Energy Procedia, 2015, 79: 73-81. DOI: 10.1016/j.egypro.2015.11.480.

[2] Yang Z, Deng B, Deng M, et al. An overview of chassis dynamometer in the testing of vehicle emission[J/OL]. MATEC Web of Conferences, 2018, 175: 02015. DOI: 10.1051/matecconf/201817502015.

[3] Öberg P, Nyberg P, Nielsen L. A new chassis dynamometer laboratory for vehicle research[J/OL]. SAE International Journal of Passenger Cars – Electronic and Electrical Systems, 2013, 6 (1): 152-161. DOI: 10.4271/2013-01-0402.

[4] Mayyas A, Prucka R, Pisu P, et al. Chassis dynamometer as a development platform for vehicle hardware in-the-loop 'VHiL'[J/OL]. SAE International Journal of Commercial Vehicles, 2013, 6(1): 257-267. DOI: 10.4271/2013-01-9018.

[5] Karra P, Jansson O. A cost-effective laboratory setup for engine and chassis-dynamometer[C/OL]// 2019 ASEE Annual Conference & Exposition Proceedings. Tampa, Florida: ASEE Conferences, 2019: 31951. DOI: 10.18260/1-2--31951.

[6] Alhanouti M, Gauterin F. Thorough analysis of the reliability of measurements on chassis roller dynamometer and accurate energy consumption estimation for electric vehicles[J/OL]. Energies, 2023, 16(24): 7994. DOI: 10.3390/en16247994.

[7] Lourenço M A D M, Eckert J J, Silva F L, et al. Vehicle and twin-roller chassis dynamometer model considering slip tire interactions[J/OL]. Mechanics Based Design of Structures and Machines, 2023, 51(11): 6166-6183. DOI: 10.1080/15397734.2022.2038199.

[8] Mate N R, Dhande D Y. Design and development of two wheeler retarder type dynamometer portable test platform[J/OL]. International Journal of Engineering Research, 2014, 3(2). DOI: 10.17577/IJERTV3IS20630.

[9] Hassan M H, Sapee S, Nafiz D M, et al. Chassis dynamometer for electric two wheelers[J/OL]. MATEC Web of Conferences, 2018, 225: 03016. DOI: 10.1051/matecconf/201822503016.

[10] Kothale S, Jagtap V P, Choudhari C S. Design of chassis dynamometer for light motor vehicle of service stations[J]. International Research Journal of Engineering and Technology (IRJET), 3(4).

[11] Kim C, Lee H, Park Y, et al. Study on the criteria for the determination of the road load correlation for automobiles and an analysis of key factors[J/OL]. Energies, 2016, 9(8): 575. DOI: 10.3390/en9080575.

[12] Gorelov V A, Komissarov A I, Sekletina L S, et al. A control algorithm for simulation of real-world operating conditions for the drivetrain of an all-wheel drive vehicle with individually driven wheels on a chassis dynamometer[J/OL]. Cogent Engineering, 2020, 7(1): 1737449. DOI: 10.1080/23311916.2020.1737449.

[13] Srivastava N, Haque I. A review on belt and chain continuously variable transmissions (CVT): Dynamics and control[J/OL]. Mechanism and Machine Theory, 2009, 44(1): 19-41. DOI: 10.1016/j.mechmachtheory.2008.06.007.

[14] Seelan V. Analysis, design and application of continuously variable transmission (CVT)[J]. 2015, 5(3).

[15] International Organization for Standardization. Road vehicles – brake lining assemblies – inertia dynamometer test method: ISO 11157:2005[S/OL]. International Organization for Standardization, 2005. https://www.iso.org/standard/36952.html.

[16] MAHA SE & Co. KG. Technical datasheet MSR 400: VP 630012[M/OL]. Haldenwang, Germany: MAHA SE & Co. KG, 2025. https://www.maha.de/restriction/check-asset/support_documents/dokumente/Brosch%C3%BCren/MAHA/04_Leistungsmesstechnik/Leistungspr%C3%BCfst%C3%A4nde/MSR/TD_MAHA_MSR_400_VP630012_en.pdf.